Electrocatalytic Effects for the Reduction of Thionyl Chloride in Li/$SOCl_2$ Cell Containing Schiff Base Metal (II) Complexes

Woo-Seong Kim,† Kwang-il Chung, Shin-Kook Kim, Seungwon Jeon, Yeon-Hee Kim, Yung-Eun Sung,† and Yong-Kook Choi*

Department of Chemistry and RRC/HECS, Chonnam National University, Kwangju 500-757, Korea
†Department of Materials Science & Engineering, K-JIST, Kwangju 500-712, Korea
Received September 27, 1999

Electrocatalytic effects for the reduction of thionyl chloride in $LiAlCl_4/SOCl_2$ electrolyte solution containing Schiff base M(II) (M; Co and Fe) complexes are evaluated by determining kinetic parameters with cyclic voltammetry and chronoamperometry at a glassy carbon electrode. The charge transfer process during the reduction of thionyl chloride is affected by the concentration of the catalyst. The catalytic effects are demonstrated from both a shift of the reduction potential for the thionyl chloride toward a more positive direction and an increase in peak currents. Catalytic effects are larger in thionyl chloride solutions containing the binuclear [$M(II)_2$(TSBP)] complex rather than mononuclear [M(II)(BSDT)] complexes. Significant improvements in the cell performance have been noted in terms of both thermodynamics and activation energy for the thionyl chloride reduction. The activation energy calculated from the Arrhenius plots is 4.5-5.9 kcal/mole at bare glassy carbon electrodes. The activation energy calculated for the catalyst containing solution is 3.3-4.9 kcal/mole, depending on whether the temperature is lowered or rasied.

Introduction

The performance of electrochemical studies for the lithium/thionyl chloride primary batteries has been of significant practical interest over the past several years and the mechanism of the reduction of thionyl chloride on various types of carbon electrodes have been studied.[1~14] The system consists of a Li anode, a porous carbon cathode, and a $LiAlCl_4/SOCl_2$ electrolyte solution, where $SOCl_2$ acts as both a solvent and a cathode-active material. The Li anode is prevented from reacting with $SOCl_2$ by virtue of the formation of a LiCl passivation film[3] on the Li as soon as it contacts the $LiAlCl_4/SOCl_2$ electrolyte according to the reaction (1).

$$4Li + 2SOCl_2 \rightarrow S + SO_2 + 4LiCl \quad (1)$$

The electrode kinetics of the cathode discharge reaction is rather poor due to the formation of passive LiCl films at the cathode as a result of reaction (1).

The film is also the source of the voltage delay owing to its overly passive nature. Many investigators tried to avoid this high passivity problem. One approach to the enhancement of cell performance can be the addition of catalyst molecules, which accelerate the rate of electron transfer.

Doddapaneni,[13,14] after comparing several metal compounds as possible catalysts, found cobalt and iron phthalocyanines to be the most effective. It also has been shown that adding a small amount of metal phthalocyanines improves cell performance by changing both thermodynamic and kinetic parameters for the thionyl chloride reduction. Choi and coworkers[11,12] have observed the passivation and catalytic of the thionyl chloride solution containing cobalt phenylporphyrins. In this paper, catalytic effects and temperature effects for the thionyl chloride reduction are reported by evaluating electrokinetic parameters in $LiAlCl_4/SOCl_2$ solution containing quadridentate Schiff base M(II) compounds as catalysts.

Experimental Section

Salicylaldehyde (Aldrich), 3,4-diaminotoluene (Aldrich), 3,3′-diaminobenzidine (Aldrich), Na_2CO_3, $Fe(SO_4) \cdot 7H_2O$, $Co(SO_4) \cdot 4H_2O$, NaOH (Aldrich), and ethanol (Aldrich) were used as received. The elemental analysis (carbon, hydrogen, and nitrogen) was performed on a Yanaco-CHN coder MT-3 analyzer, and the metal content was determined by a Perkin-Elmer model 603 atomic absorption spectrometer. ^{1}H NMR spectra in DMSO-d_6 were recorded by a Bruker AMX-300 spectrometer. Infrared and UV-vis spectra were recorded on Shimadzu IR-430 infrared and Hitachi-557 UV-vis spectrophotometers. Thermogravimetric analysis (TGA) was carried out using a Perkin-Elmer model 2 Thermogravimetric Analyzer. The molar conductance was measured in DMF at 25 °C by DKK model AO-6 Digital conductometer.

Preparation of 3,3′,4,4′-tetra(salicylidene imino)-1,1′-biphenyl; [H_4TSBP]. The quadridentate Schiff base ligands were synthesized according to the procedure in our previous report.[15,16] A 0.05 mole of the 3,3′-diaminobenzidine solution in ethanol (50 mL) was slowly added to 0.1 mole of salicylaldehyde in ethanol (50 mL) under the nitrogen atmosphere. A reddish solid [H_4TSBP] was precipitated. The precipitate was recrystallized from ethanol and dried under the reduced pressure at 80 °C: 83% yield; mp. 127-129 °C; anal. calcd. for $C_{40}H_{30}N_4O_4$: C, 76.18, H, 4.79, N, 8.88; found: C; 76.25, H, 4.83, N, 8.79; UV-vis/(DMSO, λ_{max}, $\varepsilon \times 10^{-4}$ cm^{-1} M^{-1}): 274/(4.55), 333/(3.89); IR/(KBr pellet, cm^{-1}): 3452/(OH), 3055/(C-H), 1624/(C=N), 1479/(C=C), 1190/(C-O). ^{1}H NMR/(DMSO-d_6, δ): 3.34-2.00/(10H, C_5H_{10}), 7.75-6.68/(12H, ArH), 8.91/(2H, CH=N), 12.16/(2H, $\underline{H}OC_{10}H_6$).

Preparation of 3,4-bis(salicylidene diimine) toluene; [H_2BSDT]. A 0.1 mole of 3,4-diaminotoluene solution in ethanol (50 mL) was slowly added to 0.1 mole of salicylaldehyde in ethanol (50 mL) under the nitrogen atmosphere. A yellow solid H_2BSDT was precipitated. The precipitate was recrystallized from ethanol and dried under the reduced pressure at 80 °C: 85% yield; mp. 127-130 °C; anal. calcd. for $C_{21}H_{18}N_2O_2$: C, 76.38, H, 5.45, N, 8.48, found: C, 76.29, H, 5.52, N, 8.50, UV-vis/(DMSO, λ_{max}, $\varepsilon \times 10^{-4}$cm^{-1}M^{-1}): 272/(2.37), 336/(2.19); IR/(KBr pellet, cm^{-1}): 3430/(OH), 3030/(C-H) 1620/(C=N), 1495/(C=C), 1178/(C-O). ^{1}H NMR/(DMSO-d_6, δ): 2.41/(-CH_3), 7.83-6.82/(6H, ArH), 8.92/(2H, CH=N), 12.89-13.1/(2H, $\underline{H}OC_6H_6$).

Preparation of complexes. The [M(II)$_2$(TSBP)] and [M(II)(BSDT)] complexes (M: Co, Fe) were prepared by the addition of 0.01 mole ligands in ethanol to the same volume of 0.02 mole and 0.01 mole M(II)(SO_4), respectively, in water under the nitrogen atmosphere while stirring. The M(II) complexes were precipitated. These complexes were recrystallized from ethanol and dried at 80 °C under the reduced pressure.

[Fe(II)$_2$(TSBP)]. 84% yield; mp. 175-177 °C; anal. calcd. for $C_{40}H_{24}N_4O_4Fe_2$:C, 64.89; H, 4.08; N, 7.57; Fe, 15.09; found: C, 64.91, H, 4.05, N, 7.54, Fe, 15.02, UV-vis/(DMF, λ_{max}, $\varepsilon \times 10^{-4}$ cm^{-1}M^{-1}): 412/(1.23), 472/(0.75); IR/(KBr pellet, cm^{-1}): 3049/(C-H), 1607/(C=N), 1437/(C=O), 1198/(C-O), 842/(Fe-N), 537/(Fe-O); TGA/(weight loss, %): 7.32 at 100-210 °C, 70.31 at 210-590 °C, 22.37 at 590 °C~; molar conductance/(DMF, ohm^{-1}cm^{-2}mol^{-1}): 1.42.

[Fe(II)(BSDT)]. 81% yield; mp. 187-189 °C; anal. calcd. for $C_{21}H_{16}N_2O_2Fe$: C, 65.67, H, 4.17, N, 7.29, Fe, 14.54, found: C, 65.72, H, 4.14, N, 7.34, Fe, 14.50, UV-vis/(DMSO, λ_{max}, $\varepsilon \times 10^{-4}$cm^{-1}M^{-1}): 379/(3.15), 435/(2.32); IR/(KBr pellet, cm^{-1}): 2930/(C-H), 1598/(C=N), 798/(Fe-N), 565/(Fe-O); TGA/(weight loss, %): 8.50 at 80-270 °C, 73.7 at 270-620 °C, 17.8 at 620 °C~; molar conductance/(DMF, Λ ohm^{-1}cm^{-2}mol^{-1}): 1.47.

[Co(II)$_2$(TSBP)]. 86% yield; mp. 175-177 °C; anal. calcd. for $C_{40}H_{24}N_4O_4Fe_2$: C, 64.89, H, 4.08, N, 7.57, Fe, 15.09, found: C, 64.91, H, 4.05, N, 7.54, Fe, 15.02, UV-vis/(DMF, λ_{max}, $\varepsilon \times 10^{-4}$cm^{-1}M^{-1}): 412/(1.23), 472/(0.75); IR/(KBr pellet, cm^{-1}): 3049/(C-H), 1607/(C=N), 1437/(C=O), 1198/(C-O), 842/(Fe-N), 537/(Fe-O); TGA/(weight loss, %): 7.32 at 100-210 °C, 70.31 at 210-590 °C, 22.37 at 590 °C~; molar conductance/(DMF, Λ ohm^{-1}cm^{-2}mol^{-1}): 1.42.

[Co(II)(BSDT)]. 83% yield; mp. 187-189 °C; anal. calcd. for $C_{21}H_{16}N_2O_2Fe$: C, 65.67, H, 4.17, N, 7.29, Fe, 14.54, found: C, 65.72, H, 4.14, N, 7.34, Fe, 14.50, UV-vis/(DMSO, λ_{max}, $\varepsilon \times 10^{-4}$cm^{-1}M^{-1}): 379/(3.15), 435/(2.32); IR/(KBr pellet, cm^{-1}): 2930/(C-H), 1598/(C=N), 798/(Fe-N), 565/(Fe-O); TGA/(weight loss, %): 8.45 at 80-270 °C, 73.7 at 270-620 °C, 17.85 at 620 °C~; molar conductance/(DMF, Λ ohm^{-1}cm^{-2}mol^{-1}): 1.47.

Electrochemistry. Electrochemical reduction of thionyl chloride has been carried out by cyclic voltammetry and chronoamperometry. A jacketed single compartment cell housing a glassy carbon working (geometric area, 0.071 cm^2), platinum wire counter, and lithium wire reference electrodes was used for electrochemical measurements. The glassy carbon electrode was polished to a mirror finish with 1 μm alumina powder, subsequently cleaned in an ultrasonic cleaning bath for removal of solid particles, and finally rinsed several times with doubly distilled deionized water before use. The 1.53 M $LiAlCl_4/SOCl_2$ electrolytic solution (LITHCO) was used. All experiments were conducted in a glove box under the argon-gas atmosphere. A Princeton Applied Research (PAR) 273 potentiostat/galvanostat interfaced with a microcomputer through an IEEE-488 bus was used for electrochemical measurements.

Results and Discussion

Quadridentate Schiff base metal(II) complexes were prepared and characterized by UV-vis, IR, NMR, TGA, and elemental analysis. The results of elemental analysis of the Schiff base ligands and their complexes are in good agreement with the expected composition of the proposed complexes (Scheme 1). All complexes are insoluble in water but soluble in aprotic solvents and $SOCl_2$. The results of conductivity measurements in 1 mM DMF solution indicate that the M(II) complexes are nonionic compounds. The positive charges of M(II) are perhaps neutralized by two phenoxy groups.

The IR spectra show broad ν(OH) bands of the free ligands at 3400 cm^{-1}. All of the IR spectra of M(II) complexes show typical bands of the Schiff base with strong peaks assigned to ν(C=N) in the 1598-1607 cm^{-1} region. We can see that ν(C=N) bands in the complex are shifted to the lower energy regions of 15-20 cm^{-1} in the corresponding free ligands. According to Ueno and Martell,[17] characteristic absorption bands for M(II)-N and M(II)-O bonds in complexes appear respectively in the spectral region of 650-850 cm^{-1} and 400-600 cm^{-1}. Here two absorption bands at 720-800 cm^{-1} and 540-570 cm^{-1} are assigned to be M(II)-N and

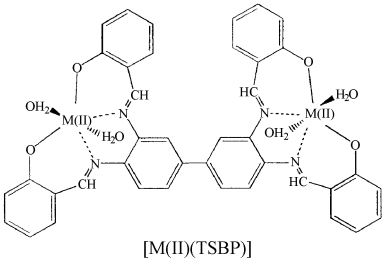

[M(II)(TSBP)]

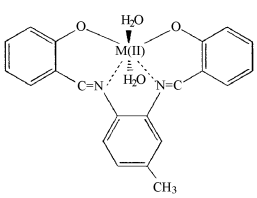

[M(II)(BSDP)]
[M : Co(II), Fe(II)]

Scheme 1

M(II)-O bonds. The UV-vis spectra of the M(II) complexes obtained in DMSO show a π-π^* ligand field absorption band at 379-412 nm and a d-π^* charge transfer band at 435-472 nm.

^{1}H NMR spectra of Schiff base ligands in DMSO-d_6 show the aromatic protons as multiples in the range 6.8-7.8 ppm and O-H protons of the two phenolic groups in the range 12.9-13.1 ppm. The spectra of Schiff base protons appear at 8.9 ppm. All M(II) complexes show the TGA curve decreasing in weight at 210-270 and with subsequent decomposition. Thermal gravimetric analysis data support that the M(II) complexes contain two or four water molecules.

Catalytic activity for electrochemical reduction of thionyl chloride by metal phthalocyanines has been demonstrated by Doddapaneni.[14] Doddapaneni reported two voltammetric peaks for the reduction of thionyl chloride in the presence of these catalysts and ascribed the catalytic activity to the formation of an adduct of thionyl chloride with a phthalocyanine molecule, followed by a two step fast electron transfer to the adduct. The two consecutive electron transfer reactions were described as

$$\text{M-Pc SOCl}_2 + e^- \rightarrow \text{M-Pc·SOCl}^\bullet + \text{Cl}^- \quad (2)$$

$$\text{M-Pc·SOCl}^\bullet + e^- \rightarrow \text{M-Pc} + 1/2\text{S} + 1/2\text{SO}_2 + \text{Cl}^- \quad (3)$$

which explain the two-voltammetric peaks observed.

Bernstein and Lever[18] described the reaction as a typical catalytic EC' reaction after running an extensive number of experiments in 1,2-dichlorobenzene. Thus, two cyclic voltammetric peaks observed during the catalytic reduction Co(III)-Pc to Co(II)-Pc first and then to Co(I)-Pc. The overall catalytic cycle is

$$\text{Co(III)-Pc} + 2e^- \ \text{Co(I)-Pc}$$
$$\text{Co(I)-Pc} + \text{SOCl}_2 \rightarrow \text{Co(III)-Pc} + 1/2\text{S} + 1/2\text{SO}_2 + 2\text{Cl}^- \quad (4)$$

These investigators have shown convincingly that $SOCl_2$ oxidizes Co(I)-Pc through a two-electron transfer reaction.

Bernstein and Lever's conclusion of the thermodynamic and kinetic requirements for electrocatalysts show that the thermodynamic reduction potential of the $SOCl_2$ must be more positive than the oxidation potentials of metal phthalocyanines and also that the electron transfer kinetics must be more favorable at a given electrode for these compounds than for thionyl chloride. While the thermodynamic requirement depends on the electron affinity of the central metal ion of a catalyst molecule, the latter would be met easily, by considering that most metal phthalocyanines are known to undergo reversible reactions due to their favorable molecular sizes as well as molecular geometry.

Catalytic effects of [M(II)$_2$(TSBP)] and [M(II)(BSDT)] complexes on the reduction of thionyl chloride at a glassy carbon electrode were evaluated by determining the kinetic parameters using cyclic voltammetry. Peak currents and peak potentials obtained from the cyclic voltammograms are plotted as a function of the catalyst concentration for

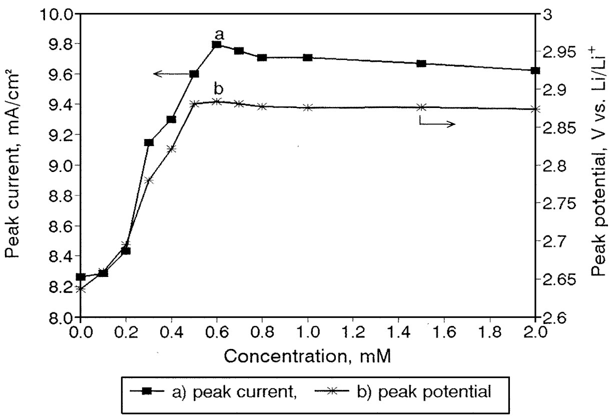

Figure 1. Plots of peak currents and peak potentials *vs*. the concentration of the catalyst for the reduction of $SOCl_2$ solution containing [Fe(II)$_2$(TSBP)] at 293 K: a) peak current and b) peak potential. Scan rate was 50 mV/sec.

[M(II)$_2$(TSBP)] complex as shown in Figure 1. The magnitude of the reduction current appears to be dependent on the catalyst concentration in the thionyl chloride solution. These phenomena are observed for all complexes, although the extent of the effects is different. There is an optimum concentration for each catalyst at around 0.6-0.7 mM because the rate-limiting step for reduction of the thionyl chloride depends on the electron transfer at the electrode surface.

Figure 2 shows cyclic voltamograms of thionyl chloride reduction in the presence of the optimum concentration of [M(II)$_2$(TSBP)] and [M(II)(BSDT)] complexes at a glassy carbon electrode. As shown in Figure 2, a sharp current drop at a less positive side seems to be due to passivation of the electrode by lithium chloride.[7] The catalytic effects are clearly seen by both the shift of the reduction potential for thionyl chloride towards a positive direction, resulting in the decrease of the overpotential. This indicates that Schiff base complexes used in this study behave as catalysts for the reduction of thionyl chloride. Therefore, we conclude that these

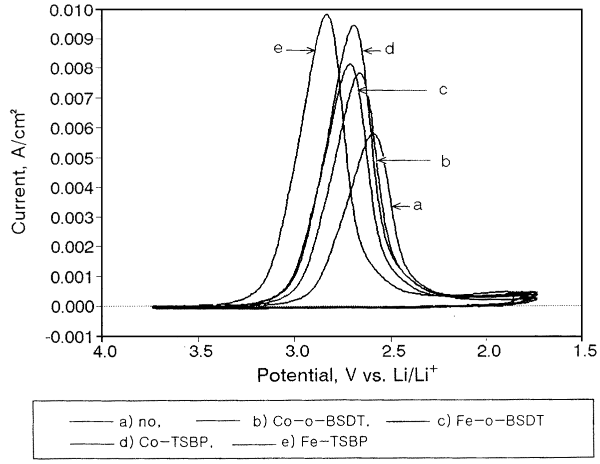

Figure 2. Cyclic voltammograms for the reduction of $SOCl_2$ solution at optimum concentrations containing: a) no, b) [Co(II)-(BSDT)], c) [Co(II)$_2$(TSBP)], d) [Fe(II)(BSDT)], and e) [Fe(II)$_2$-(TSBP)]. Scan rate was 50 mV/s.

Table 1. [a]Peak potentials for the reduction of thionyl chloride at scan rate of 50 mV/sec

Catalyst	Temperature (K)					
	303	293	283	273	263	253
Bare	2.66	2.64	2.61	2.51	2.46	2.41
Co(II)(BSDT)	2.76	2.71	2.66	2.63	2.61	2.60
Fe(II)(BSDT)	2.83	2.76	2.68	2.62	2.58	2.53
$Co(II)_2$(TSBP)	2.76	2.74	2.68	2.64	2.60	2.56
$Fe(II)_2$(TSBP)	2.96	2.88	2.80	2.74	2.68	2.62

[a]peak potential obtained from cyclic voltammetry, V *vs.* Li/Li^+.

Table 2. [a]Peak currents for the reduction of thionyl chloride at scan rate of 50 mV/sec

Catalyst	Temperature (K)					
	303	293	283	273	263	253
Bare	5.81	5.18	4.62	4.57	3.41	2.39
Co(II)BSDT	8.84	7.83	7.63	6.42	4.94	3.72
Fe(II)BSDT	8.29	8.12	7.58	7.69	5.59	4.64
$Co(II)_2$TSBP	9.51	9.44	9.27	8.12	7.12	5.37
$Fe(II)_2$TSBP	10.09	9.79	9.44	8.53	7.64	6.63

[a]peak current obtained from cyclic voltammetry, mA/cm^2.

compounds show good catalytic activities at a glassy carbon electrode. These results are in accordance with previous results reported by Doddapaneni[13] on the reduction of the $SOCl_2$ solution containing metal phthalocyanine.

An extensive number of cyclic voltammetric experiments only at the "optimum" catalyst concentration was conducted to evaluate kinetic parameters at different temperatures. From these results, the peak currents and potentials observed for the reduction of thionyl chloride at different temperatures are summarized in Tables 1 and 2. Figure 3 shows a series of cyclic voltammograms recorded at various scan rates in thionyl chloride solution containing 0.68 mM $[Fe(II)_2(TSBP)]$. The current decays faster than the Cottrellian fashion beyond the cyclic voltammogram peak potential. As discussed above, these phenomena seem to be due to some passivation of the electrode surface during the reduction of thionyl chloride. To establish, whether the electron transfer is a diffusion-controlled or surface process, cyclic voltammetric peak currents are plotted against scan rates. Figure 4 shows a plot of peak current *vs.* $v^{1/2}$ (v: scan rate) from voltammetric results obtained at the glassy carbon electrode under "optimum" conditions. The result of the plots in Figure 4 indicates that the thionyl chloride reduction at the glassy carbon electrode is controlled by diffusion of the electroactive compound. The peak current from cyclic voltammetry for an irreversible case is given as follows.[19]

$$i_p = (2.99 \times 10^5) n(\alpha n_a)^{1/2} A C_o^* D_o^{1/2} v^{1/2} \quad (5)$$

where n is the number of electrons transferred, α is the transfer coefficient, n_a is the apparent number of electrons transferred, A is the electrode area in cm^2, C_o^* is the bulk concentration of an electroactive compound in $mole/cm^3$, and D_o is the diffusion coefficient of the electroactive compound or other charge carrier in cm^2/sec. Eq. (5) reveals that a plot of i_p *vs.* $v^{1/2}$ allows us to obtain the diffusion coefficient of thionyl chloride with known αn_a. From the relationship of i_p with E_p[19]

$$i_p = 0.227 nFAC_o^* k^o \exp[-\{(\alpha n_a F)/(RT)\}(E_p - E^{o'})] \quad (6)$$

where k^o is the exchange rate constant in cm/sec and $E^{o'}$ is the standard electrode potential in V, we can calculate k^o. A plot of $\ln(i_p)$ *vs.* $E_p - E^{o'}$ should yield a straight line with a slope, $\alpha n_a F/RT$, and an intercept, $\ln(0.227 nFAC_o^* k^o)$, from which n_a and k^o values can be calculated, respectively. In these calculations, the thermodynamic E^o, value of 3.72 V *vs.* Li is used as it is obtained from Eq. (1) using free energies of formation for reactants and products.[6] The $\ln(i_p)$ *vs.* $(E_p - E^{o'})$ plots are shown in Figure 5 for the reduction of $SOCl_2$ at the glassy carbon electrode. The αn_a value obtained from this equation can be used to determine $AD_o^{1/2}$ in Eq. (5).

Kinetic parameters calculated from these plots at "optimum" catalyst concentrations are listed in Table 3. As

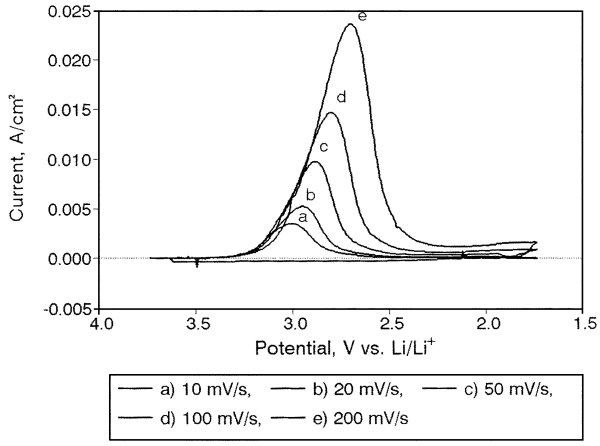

Figure 3. Scan rate dependency of the voltammograms for the reduction of the $SOCl_2$ solution containing 0.68 mM $[Fe(II)_2$-(TSBP)] at 293 K. Scan rates were. a) 10, b) 20, c) 50, d) 100, and e) 200 mV/s.

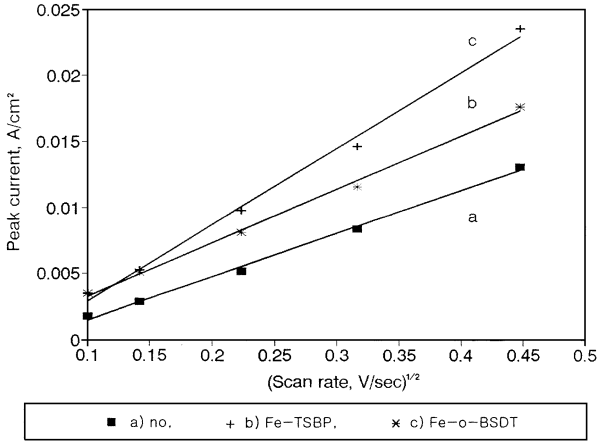

Figure 4. Plots of current *vs.* $v^{1/2}$ for the reduction of $SOCl_2$ at optimum concentrations containing: a) no, b) $[Fe(II)_2(TSBP)]$, and c) [Fe(II)(BSDT)].

Table 3. Kinetic parameters for the reduction of thionyl chloride

Temp. (K)		Catalyst				
		Bare	Co(II)BSDT	Fe(II)BSDT	$Co(II)_2$TSBP	$Fe(II)_2$TSBP
303	αn_a	0.17	0.19	0.19	0.19	0.18
	AD_0	2.50×10^{-8}	4.54×10^{-8}	4.40×10^{-8}	6.56×10^{-8}	7.85×10^{-8}
	k^0	9.59×10^{-8}	1.58×10^{-7}	2.32×10^{-7}	1.01×10^{-7}	1.42×10^{-6}
293	αn_a	0.18	0.20	0.19	0.21	0.16
	AD_0	1.81×10^{-8}	3.83×10^{-8}	3.96×10^{-8}	5.44×10^{-8}	6.82×10^{-8}
	k^0	4.46×10^{-8}	4.37×10^{-8}	8.63×10^{-8}	4.19×10^{-8}	5.38×10^{-7}
283	αn_a	0.19	0.20	0.20	0.20	0.16
	AD_0	1.59×10^{-8}	3.30×10^{-8}	3.67×10^{-8}	4.18×10^{-8}	5.46×10^{-8}
	k^0	1.88×10^{-8}	2.47×10^{-8}	3.05×10^{-8}	2.50×10^{-8}	2.80×10^{-7}
273	αn_a	0.19	0.20	0.20	0.20	0.16
	AD_0	9.56×10^{-9}	2.48×10^{-8}	3.30×10^{-8}	4.04×10^{-8}	4.86×10^{-8}
	k^0	5.85×10^{-9}	1.19×10^{-8}	1.19×10^{-8}	1.02×10^{-8}	9.88×10^{-8}
263	αn_a	0.18	0.20	0.21	0.21	0.16
	AD_0	7.43×10^{-9}	1.61×10^{-8}	2.04×10^{-8}	2.86×10^{-8}	3.48×10^{-8}
	k^0	2.07×10^{-9}	5.07×10^{-9}	2.85×10^{-9}	4.43×10^{-9}	4.73×10^{-8}
253	αn_a	0.19	0.21	0.19	0.21	0.17
	AD_0	5.13×10^{-9}	1.11×10^{-8}	8.29×10^{-9}	1.59×10^{-8}	2.03×10^{-8}
	k^0	6.85×10^{-10}	1.53×10^{-9}	1.55×10^{-9}	1.47×10^{-9}	1.24×10^{-8}

shown in Table 3, exchange rate constants, k^o, are determined to be 4.46×10^{-8} cm/s at the bare glassy carbon electrode at 293 K. On the other hand, these values are determined to be 5.38×10^{-7}~4.19×10^{-8} m/s at the catalyst supported glassy carbon electrode. The increase in exchange rate constant indicates significant improvements in cell performance. Therefore most of the enhancement is attributed to the catalytic effects of the Shciff base complexes.

We also carried out chronoamperometric experiments for reduction of $SOCl_2$ in order to estimate the diffusion coefficient. Figure 6A shows chronoamperometric curve of $SOCl_2$ solution containing 1.53 M $LiAlCl_4$ at –2.5 V *vs.* Li/Li^+. Figure 6B shows the result obtained from Cottrell equation, *i.e.*,

$$i(t) = \frac{nFAD_o^{1/2}C_o^*}{\pi^{1/2}t^{1/2}} \quad (7)$$

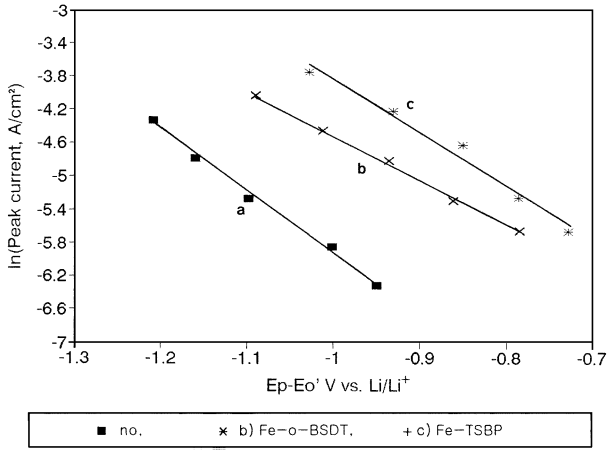

Figure 5. Plots of $\ln(i_p)$ *vs.* $(E_p-E^{o'})$ for the reduction of $SOCl_2$ at optimum concentration containing: a) no, b) [Fe(II)(BSDT)], and c) [$Fe(II)_2$(TSBP)].

Here $i(t)$ is the current at time t. Eq. (7) predicts that the plot of $i(t)$ *vs.* $t^{-1/2}$ should be linear with a slope of $nFAD_o^{1/2}C_o^*/\pi^{1/2}$. The values of diffusion coefficient calculated from the slope of Figure 6B are listed in Table 3. As can be seen in Table 3, diffusion coefficients obtained from chronoampe-

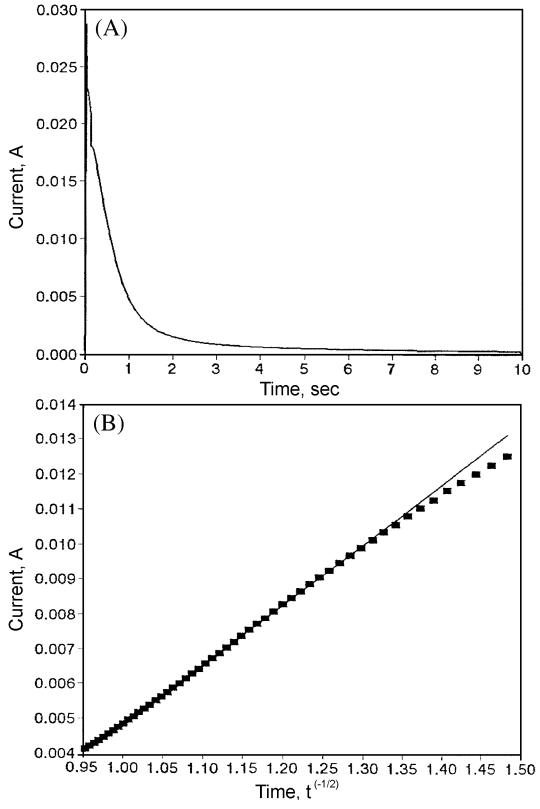

Figure 6. Chronoamperometric curve (A) and Cottrell plot (B) for reduction of $SOCl_2$ at 2.5 V *vs.* Li/Li^+ in the presence of [$Fe(II)_2$(TSBP)].

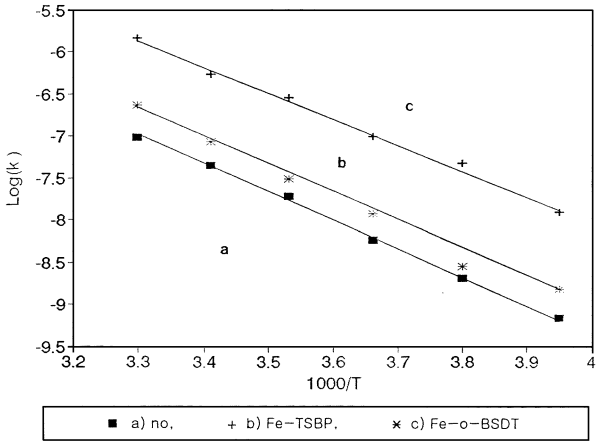

Figure 7. The Arrehenius plots for exchange rate constants obtained while temperature is lowered; a) no, b) [Fe(II)$_2$(TSBP)], and c) [Fe(II)(BSDT)].

Table 4. Activation energy for the reduction of thionyl chloride depending on whether the temperature is lowered (L) or raised (R)

Catalysts	Activation energy (kcal/mol)	
	L	R
Bare	4.51	5.89
Co(II)(BSDT)	3.74	4.69
Fe(II)(BSDT)	3.83	4.88
Co(II)$_2$(TSBP)	3.45	4.59
Fe(II)$_2$(TSBP)	3.32	4.67

rometry are consistent with those determined from cyclic voltammetry.

Exchange rate constants are affected by cell temperature. Furthermore, there is a fair amount of hysteresis present depending on whether data is obtained while the cell temperature is lowered or raised. We ran an extensive number of experiments, but hysteresis was always significant, although data were reproducible. Figure 7 shows the Arrhenius plots for the reduction of thionyl chloride. As shown in Figure 7 and Table 4, the activation energy calculated from the Arrhenius plots at bare glassy carbon electrode is 4.5 and 5.9 kcal/mole, respectively, depending on whether the temperature is lowered or raised. Also the activation energy calculated for the solution containing [M(II)$_2$(TSBP)] are 3.3 and 4.7 kcal/mole, whereas 3.7 and 4.9 kcal/mole for the solution containing [M(II)(BSDT)], respectively. We believe that the hysteresis results from different morphology and porosity of the electrode surface film as already point out.[11] Depending on whether the temperature is lowered or raised, crystal nucleation and growth rates vary, resulting in different morphology and porosity. However as shown in Table 1-3, catalytic effects are slightly larger in thionyl chloride solution containing [M(II)$_2$(TSBP)] than [M(II)(BSDT)] complexes due probably to the steric reason. Two metal sites in the [M(II)$_2$(TSBP)] catalyst seem to participate more easily in the catalytic reaction.

Conclusions

It is clear that some Schiff base transition metal compounds show sizable catalytic activity for the reduction of thionyl chloride. From our results, we conclude that:

1. the catalyst molecules are reduced on the electrode surface, which in turn reduces thionyl chloride, resulting in the generation of oxidized catalyst molecules and thus completes the catalytic cycle;
2. there is an optimum concentration for each catalyst;
3. relative catalytic effects are slightly larger in the thionyl chloride solution containing M(II)$_2$(TSBP)] compound compare with [M(II)[BSDT)].

Acknowledgment. This work was supported by the Basic Science Research Institute Program, Ministry of Education of Korea (BSRI 98-3429) and in part by the Korean Science and Engineering Foundation through the Region Research Center of HECS of Chonnam National University (1999).

References

1. Schlaikjer, C. R.; Goedel, F.; Marincic, N. *J. Electrochem. Soc.* **1976**, *126*, 513.
2. Dey, A. N.; Bro, P. *J. Electrochem. Soc.* **1978**, *125*, 1574.
3. Salmon, D. J.; Adamczyk, M. E.; Hendricks, L. L.; Abels, L. L.; Hall, J. C. In *Lithium Battery Technology*; Venkatasetty, H. V., Ed.; Proc. Electrochemical Society: Pennington, NJ., 1981.
4. Istone, W. K.; Brodd, R. J. *J. Electrochem. Soc.* **1982**, *129*, 1853.
5. Istone, W. K.; Brodd, R. J. *J. Electrochem. Soc.* **1984**, *131*, 2467.
6. Madou, M. J.; Szpak, S. *J. Electrochem. Soc.* **1984**, *131*, 2471.
7. Madou, M. J.; Smith, J. J.; Szpak, S. *J. Electrochem. Soc.* **1987**, *134*, 2794.
8. Hills, A. J.; Hampson, N. A. *J. Power Sources* **1988**, *24*, 253.
9. Mosier-Boss, P. A.; Szpak, V.; Smith, J. J.; Nowak, R. J. *J. Electrochem. Soc.* **1989**, *136*, 2455.
10. Bagotsky, V. S.; Kazarinov, V. E.; Volfkovich, Yu. M.; Kanevsky, L. S.; Beketayeva, L. A. *J. Power Sources* **1989**, *26*, 427.
11. Choi, Y. K.; Kim, B. S.; Park, S. M. *J. Electrochem. Soc.* **1993**, *140*, 11.
12. Kim, W. S.; Choi, Y. K.; Chjo, K. H. *Bull. Korean Chem. Soc.* **1994**, *15*, 456.
13. Doddapaneni, N. *Proc. 30th Power Sources Symp.*; The Electrochem. Soc. Inc.: Atlantic City, NJ., 1982; p 169.
14. Doddapaneni, N. *Proc. of the Symposium on the Chemistry and Physics of Electrocatalysis*; The Electrochem. Soc. Inc.; Pennington, NJ., 1994; p 630.
15. Choi, Y. K.; Chjo, K. H.; Park, K. H. *Bull. Korean Chem. Soc.* **1995**, *16*, 21.
16. Choi, Y. K.; Chjo, K. H.; Park, S. M.; Doddapaneri, N. *J. Electrochem. Soc.* **1995**, *142*, 4107.
17. Ueno, K.; Martell, A. E. *J. Phy. Chem.* **1956**, *60*, 1270.
18. Bernstein, P. A.; Lever, A. B. P. *Inorg. Chem.* **1990**, *29*, 608.
19. Bard, A. J.; Faulkner, L. R. *Electrochemical Methods*; Wiley: New York, 1980; Chap. 6.